Sedimentation of particles: collective effects and deformable filaments

PhD Defense

Benjamin Marchetti
Supervised by L. Bergougnoux and É. Guazzelli

26/09/2018

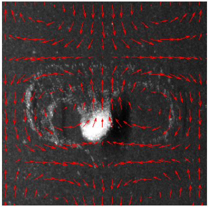

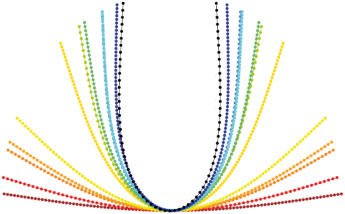

Flow of particles in industry

Figure 1: Paper industry (upper left) ; Fiber-reinforced concrete (upper right) ; Paris (2014) (middle)

Flow of particles in nature

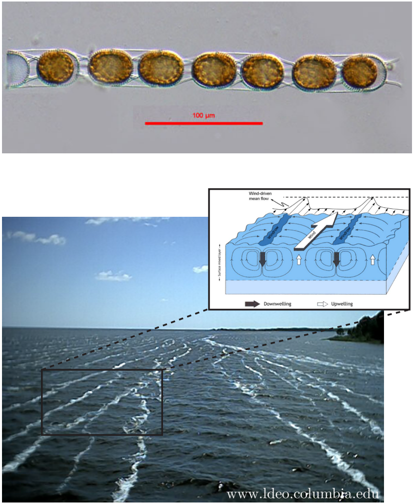

Figure 2: Stephanopyxis nipponica (**source**: Phycokey, University of New Hampshire) ; Langmuir circulation (**source**: Tejada-Martinez *et al.* (Phys. Scr., 2013))

Figure 3: Eyjafjöll, Island (**source**: British Met Office (2010))

Outline

Sedimentation of

①

Cloud of particles in vortical flow

②

Flexible fiber in a quiescent viscous fluid

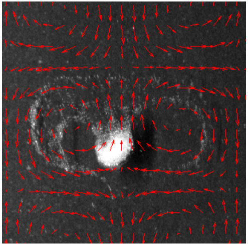

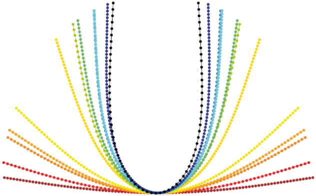

Experimental and numerical investigations

Part 1

Sedimentation of cloud of particles in a vortical flow

Collective dynamics: viscous regime ($Re_a \sim 10^{-4}$)

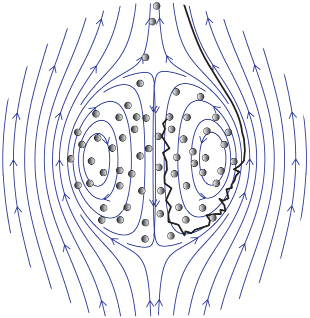

Figure 4: Flow produced by a cloud of particles (**source**: Metzger, B. and Guazzelli, E. (2008), Reflets de la physique)

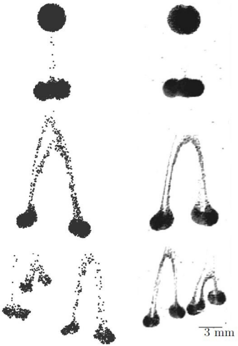

Figure 5: Snapshots of a cloud of particles settling in a quiescent fluid. (Left) Numerical simulation, (Right) Experimental (**source**: Metzger, B. *et al.* (2007), JFM)

Collective dynamics: weak inertia regime ($Re_a \sim 10^{-2}$)

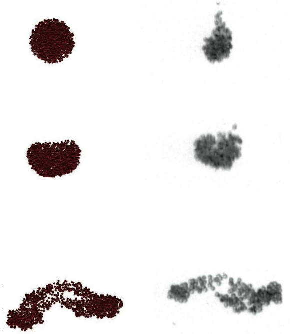

Figure 6: Snapshots of a cloud of particles settling in a quiescent fluid. (Left) Numerical simulation, (Right) Experimental (**source**: Pignatel, F. *et al.* (2011), JFM)

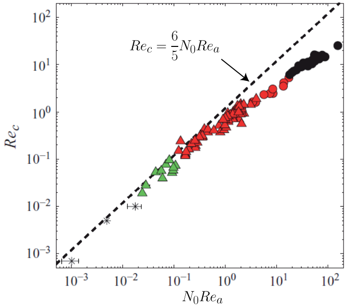

Figure 7: Re_c vs $N_0 Re_a$ (**source**: Pignatel, F. *et al.* (2011), JFM)

Dynamic in turbulent or vortical flow

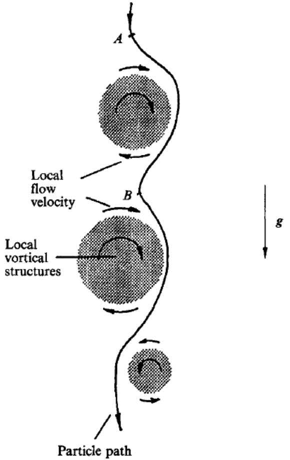

Figure 8: Sketch showing the preferential sweeping mechanism for a heavy particle interacting with local flow vortical structures. (**source**: Wang, L. and Maxey, M.R., JFM (1993))

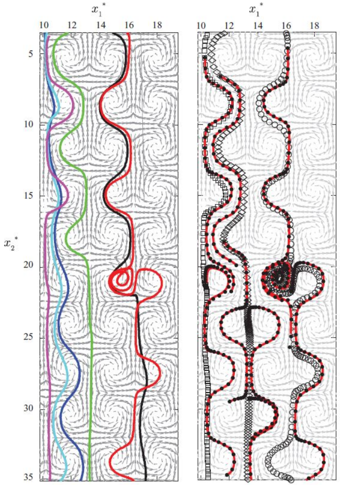

Figure 9: Experimental and numerical trajectories of a particle settling in a vortical flow (**source**: Bergougnoux, L. *et al.* (2014), PoF)

Collective dynamics in vortical flow

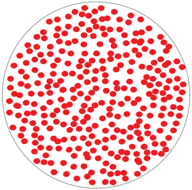

+

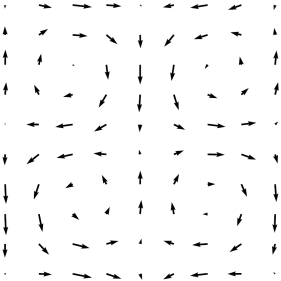

?

Deformation

Velocity

Leakage

Life-time

Dimensional analysis

Physical quantities

- Fluid: ρ_f, μ, U_0 and vortex size $k^{-1} = L/\pi$
- Particles: a and ρ_p
- Cloud: radius, R_c, and number of particles, N_0
- Gravitational acceleration g

6 independent dimensionless numbers

- Flow Reynolds number: $Re_k = \rho_f U_0 k^{-1}/\mu$
- Stokes to flow velocity ratio: $W = U_s/U_0$
- Number of particles N_0
- Particle Reynolds number: $Re_a = \rho_f U_S a/\mu$ or alternatively the dimensionless inertial length $k\ell$ or ℓ/R_c with $\ell = a/Re_a$
- Particle to vortex size ratio: $P = a/k^{-1}$ or alternatively cloud to vortex size ratio: $Q = R_c/k^{-1}$
- Stokes number, $St = \frac{2}{9}(\rho_p + \frac{\rho_f}{2})\frac{a^2 k U_0}{\mu}$, always kept small in the present experiment

Experimental setup

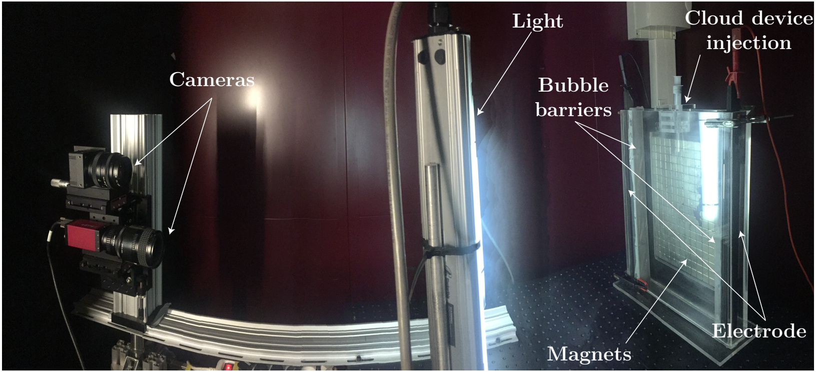

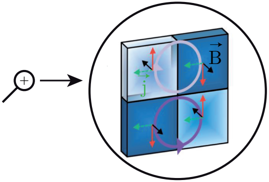

- Particles: Polystyrene ($a = 70\mu m$, $a = 115\mu m$) and PMMA particle ($a = 175\mu m$)
- 2 fluids:
  1) 83% water + 7% citric acid + 10% Ucon^{TM} oil
  2) 64% water + 36% citric acid

Tabeling *et al.*, Europhys. Lett.(1987)

Two regimes: viscous and weak inertia

Viscous regime

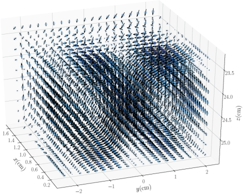

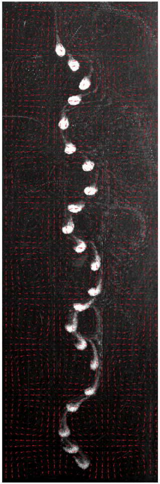

$$2200 < N_0 < 20000$$
$$2\ 10^{-3} < W < 2\ 10^{-2}$$
$$0.7 < Re_k < 2.9$$
$$Re_a \sim 10^{-4}$$
$$0.01 < P < 0.02\ ;\ 0.2 < Q < 0.4$$

Weak inertia regime

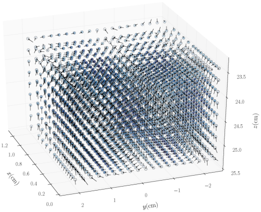

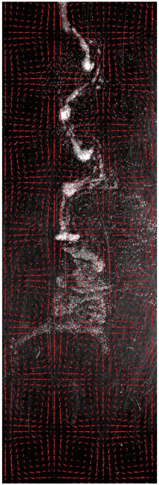

$$300 < N_0 < 700$$
$$5\ 10^{-2} < W < 10^{-1}$$
$$6.8 < Re_k < 13.6$$
$$Re_a \sim 10^{-2}$$
$$P \sim 0.03\ ;\ 0.4 < Q < 0.6$$

Numerical method: Stokeslet in viscous regime

Validity: $Re_a \ll 1$

- Linearity of equations
- Sum of interactions

A cloud of size Q with N_0 particles

$$\dot{\hat{r}}_i^{\alpha} = \hat{V}_i^{PIV}(\dot{\hat{r}}_i^{\alpha}) + W\,\delta_{i3} + \frac{3}{4}PW\sum_{\alpha\neq\beta}^{N_0-1}\left[\frac{\delta_{i3}}{\hat{r}^{\alpha\beta}} + \frac{\hat{r}_i^{\alpha\beta}\hat{r}_3^{\alpha\beta}}{(\hat{r}^{\alpha\beta})^3}\right]$$

with $P = a/k^{-1}$ and $W = U_s/U_0$

Length scale: k^{-1}, Velocity scale: U_0

Metzger *et al.*, JFM (2007)

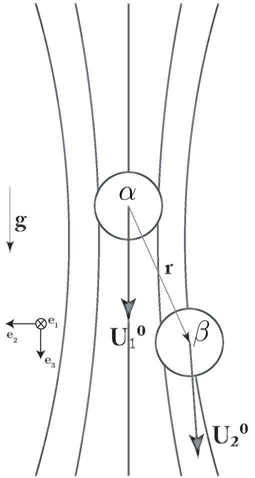

Figure 10: Two spheres settling in a quiescent viscous fluid (**source:** Guazzelli, E. and Morris, J.F., A Physical Introduction to Suspension Dynamics, *Cambridge University Press* (2011))

Numerical method: Oseenlet in weak inertia regime

A cloud of size Q with N_0 particles

$$\dot{\hat{r}}_i^{\alpha} = \hat{V}_i^{PIV}(\hat{r}_i^{\alpha}) + W\,\delta_{i3} + \frac{3}{4}PW\sum_{\alpha\neq\beta}^{N-1}\left\{\frac{\hat{r}_i^{\alpha\beta}}{(\hat{r}^{\alpha\beta})^2}\left[\frac{2\ell^*}{\hat{r}^{\alpha\beta}}(1-\hat{E})-\hat{E}\right]+\frac{\hat{E}}{\hat{r}^{\alpha\beta}}\delta_{i3}\right\}$$

$$\hat{E} = \exp\left[-\left(1+\frac{\hat{r}_3^{\alpha\beta}}{\hat{r}}\right)\frac{\hat{r}^{\alpha\beta}}{2\ell^*}\right]$$
$$\ell^* = (a/Re_a)/R_c$$

Pignatel *et al.*, JFM (2011)

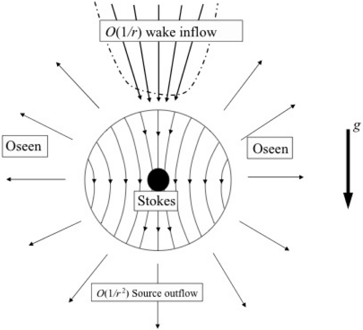

Figure 11: Oseen solution: flow around a sphere settling in a quiescent fluid at weak inertia (**source**: Subramanian and Koch, JFM (2008))

Qualitative comparisons

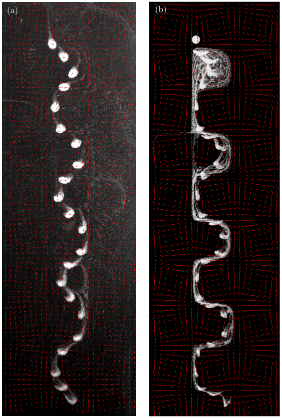

Figure 12: Viscous regime.
Experimental (a) and numerical (b) results.
$N_0 \approx 2500$, $Re_a = 10^{-4}$ and $Re_k \approx 2.9$

Motion of the cloud

The cloud tends to settle along the downstream flow regions.
→ zigzagging motions
Preferential sweeping

The cloud successively **expands** and **shrinks** when settling through the successive elongational portions of the flow.

Increasing inertia enhances the cloud deformation.

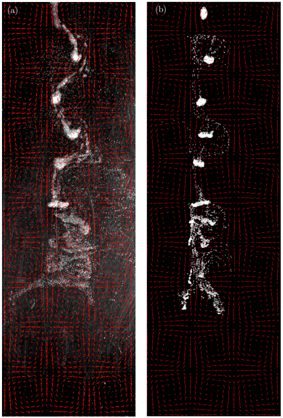

Figure 13: Weak inertia regime.
Experimental (a) and numerical (b) results.
$N_0 \approx 500$, $Re_a = 10^{-2}$ and $Re_k \approx 13.6$

Quantitative comparisons: cloud velocity and deformation

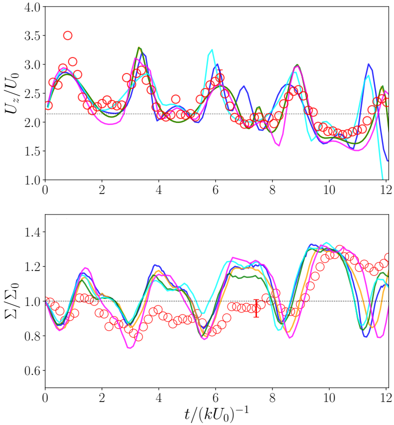

Figure 14: Viscous regime

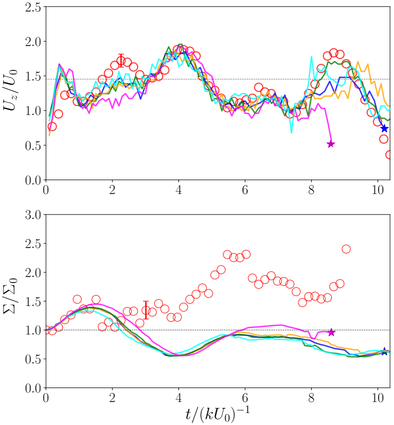

Figure 15: Weak inertia regime

Leakage of particles

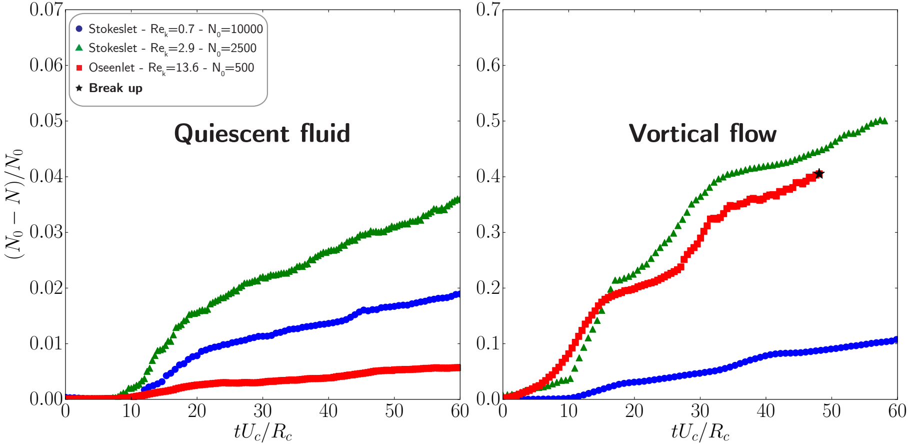

- The leakage is intensified by the vortical flows
- The leakage is amplified with inertia (using the Oseenlet modeling)

Life-time of the cloud

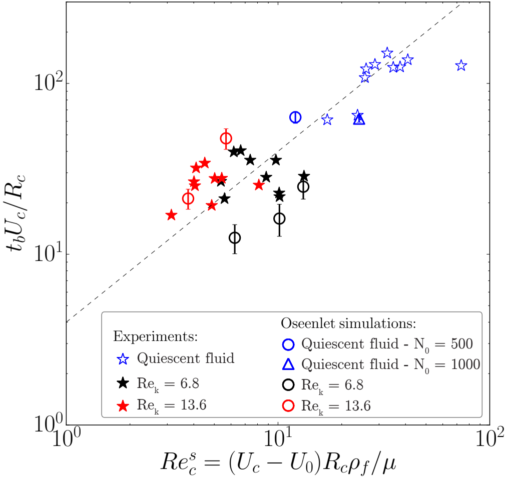

Break-up time of the cloud versus the slip Reynolds number

- The cloud life-time is reduced by the presence of vortex flows
- Increase of $t_b U_c/R_c$ with increasing Re_c^s
- Great sensitivity to the initial position and the 3D velocity field

Conclusion

- Joint experimental and numerical investigation to examine the dynamics of clouds of particles settling in cellular flows composed by counter-rotating vortices
- Success of the point-particle simulation by using Stokeslet for the viscous regime and Oseenlet for the finite inertia regime
- The cellular structure affects the cloud aspect ratio, increases particle leakage, and decreases the cloud life-time (for finite inertia)

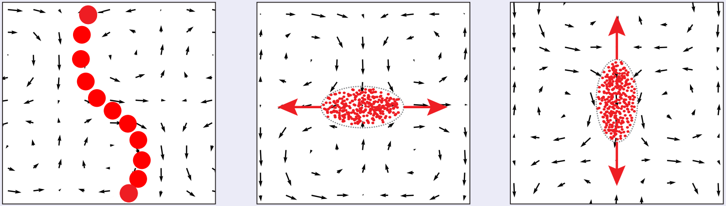

Part 2

Sedimentation of a flexible fiber in a quiescent viscous fluid

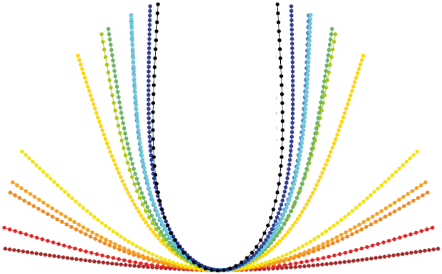

Sedimentation of a rigid fiber in viscous regime

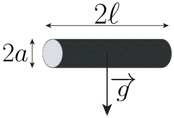

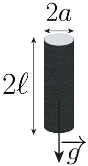

Drag force $\perp$

$$F_{\perp}^{drag} = C_{\perp}\mu U_{\perp}(2\ell)$$

$$C_{\perp} = \frac{4\pi}{ln(4\kappa^{-1}) - 1/2}$$

$$U_{\perp} = \frac{\Delta\rho g a^2[ln(4\kappa^{-1}) - 1/2]}{4\mu}$$

Drag force $\parallel$

$$F_{\parallel}^{drag} = C_{\parallel}\mu U_{\parallel}(2\ell)$$

$$C_{\parallel} = \frac{2\pi}{ln(4\kappa^{-1}) - 3/2}$$

$$U_{\parallel} = \frac{\Delta\rho g a^2[ln(4\kappa^{-1}) - 3/2]}{2\mu}$$

With,

$$\kappa^{-1} = \frac{\ell}{a} \text{ and } U_{\parallel}/U_{\perp}(\kappa^{-1}) = C_{\perp}/C_{\parallel}(\kappa^{-1}) \approx 1.5 - 1.7$$

Cox, JFM (1970)

Deformation of a flexible fiber: various types of modeling

Slender body theory

- Analytical solution for small deformation

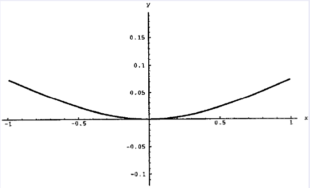

Xu and Nadim, PoF (1994)

- Numerical simulation for $\ell/a \gg 1$

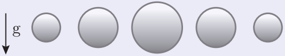

Li *et al.*, JFM (2013)

Connected beads

- String of connected bead with bending moments

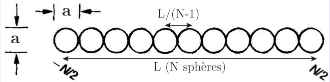

Cosentino Lagomarsino *et al.*, PRL (2005)

- Gear model

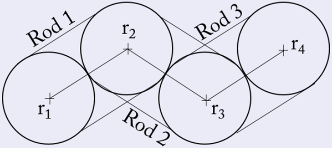

Delmotte *et al.*, J. Comp. Phys. (2015)

Dimensional analysis

Physical quantities

- Fluid: ρ_f and μ
- Fiber: a, ℓ, ρ_{fiber} and E
- Gravitational acceleration g

4 independent dimensionless numbers

- Aspect ratio $\kappa^{-1} = \ell/a$
- Elasto-gravitational number: $\mathcal{B} = \frac{Gravity\ force}{Elastic\ force} = \frac{F_G(2\ell)^2}{EI}$
  With $F_G = \Delta\rho(2\ell)\pi a^2 g$ and $I = \pi a^4/4$
  or Elasto-viscous number: $\mathcal{V} = \frac{Viscous\ force}{Elastic\ force} = \frac{\mu U(2\ell)^3}{EI}$
- Fiber Reynolds number $Re = \frac{U\ell\rho_f}{\mu} \ll 1$ or $Re_a = \frac{Ua\rho_f}{\mu} \ll 1$
- Fiber Stokes number $St_{fiber} = \frac{1}{3}\frac{a\rho_s U}{ln(\kappa^{-1})\mu} \ll 1$

Sedimentation and deformation of flexible fibers

Elasto-gravitational number

$$\mathcal{B} = \frac{Gravity\ force}{Elastic\ force} = \frac{F_G(2\ell)^2}{E\pi a^4/4}$$

with $F_G = \Delta\rho(2\ell)\pi a^2 g$

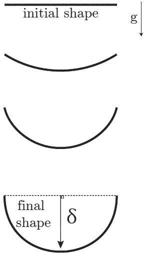

Figure 16: Definition of δ

X. Xu and A. Nadim, PoF (1994)
M. Cosentino Lagomarsino *et al.*, PRL (2005)
L. Li *et al.*, JFM (2013)
B. Delmotte *et al.*, J. Compu. Phys.(2015)

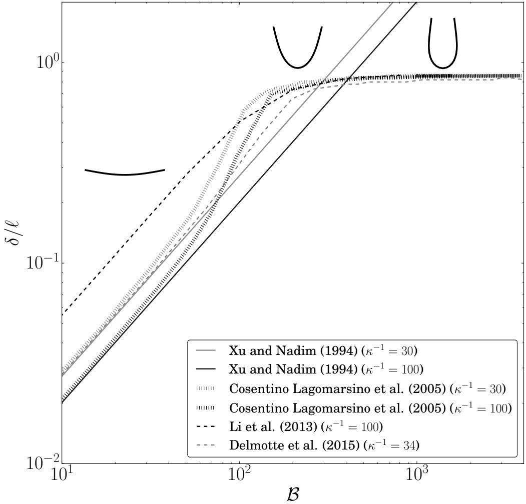

Figure 17: Amplitude of deflection depending on the value of $\mathcal{B}$

Experimental setup with V. Raspa and C. Duprat (LadHyX, Palaiseau) and A. Lindner and O. Du Roure (PMMH ,Paris)

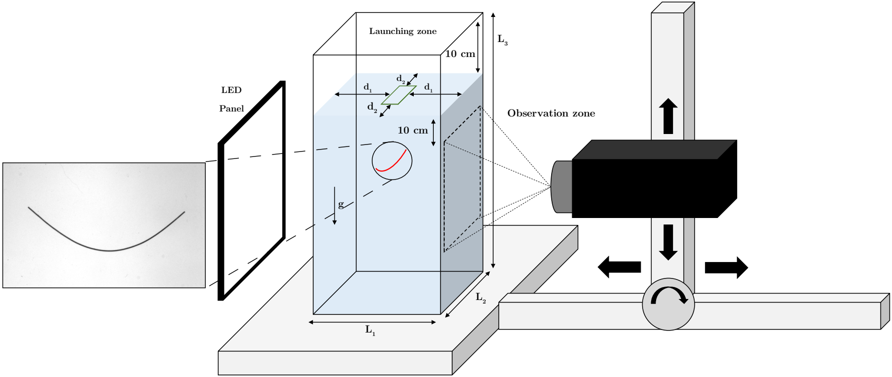

Fibers fabricated from silicon-based elastomer (Zermak Elite double 8) and iron molded in capillary tubes

$30 \lesssim \mathcal{B} \lesssim 1000$ $\quad$ $70 < \kappa^{-1} < 300$ $\quad$ $Re \lesssim 0.2$ $\quad$ $St_{fiber} < 10^{-3}$

Experimental parameters

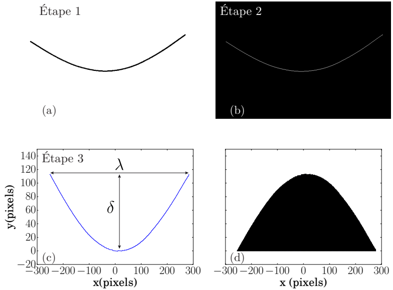

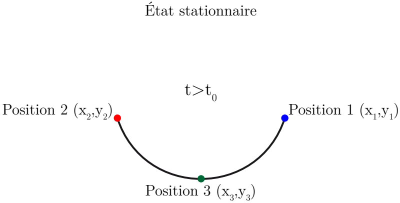

Parameters measured

- δ maximum amplitude of deflection
- λ end-to-end distance
- U velocity

Chronophotographies in the stationary state

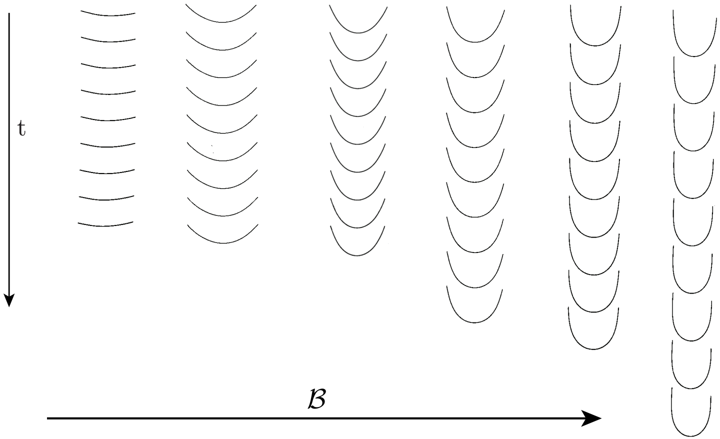

Figure 18: Flexible filaments settling in a quiescent viscous fluid for different $\mathcal{B}$; ($\mathcal{B}$ = 57; 111; 207; 222; 329; 439; 549); $\Delta t = 10a/U_\perp$. (**source**: V. Raspa and C. Duprat, LadHyX).

Bead-spring model

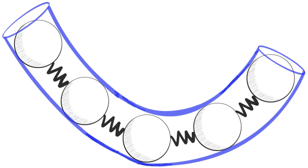

Figure 19: Sketch of a fiber

Position at each time step

$$\dot{\hat{r}}_i^\alpha = \sum_{\alpha \neq \beta}^{N-1} \hat{\mathcal{M}}_{ij}^{\alpha\beta} \left(\hat{F}_j^\beta - \varepsilon \frac{\partial \hat{\mathcal{U}}}{\partial \hat{r}_j^\beta} \right)$$

with $\varepsilon = 24\kappa^{-3}/\mathcal{B}$

- $\mathcal{M}$: mobility matrix Rotne-Prager-Yamakawa. Sum of hydrodynamic interactions of the spheres
- F^β: external force due to the gravity on each particle
- $\mathcal{U}$ elastic potential combining stretching and bending force

length scale: a and time scale: a/U_s

J. Rotne and S. Prager, J. Chem. Phys. (1969) - H. Yamakawa, J. Chem. Phys. (1970)

Comparison of amplitude

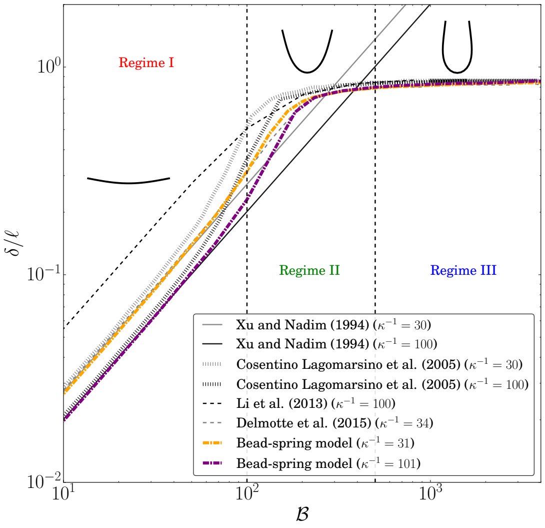

- Regime I : linear deformation with $\mathcal{B}$
- Regime II : difference observed between models in the intermediate (reconfiguration) regime
- Regime III : saturation at large $\mathcal{B}$

Chronophotographies in the stationary state

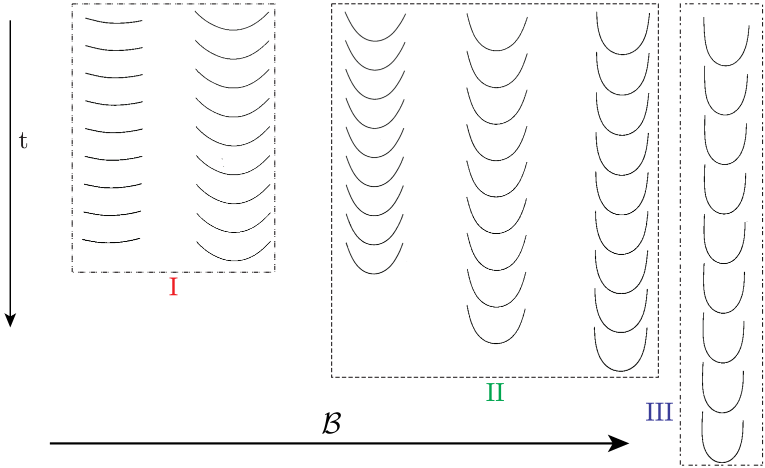

Three regimes

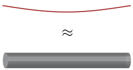

I

Weak deformation
$\mathcal{B} < 100$

$$\boxed{F_{drag} \approx C_\perp \mu U_\perp 2\ell}$$

$$\boxed{U \approx U_\perp}$$

$$\mathcal{B} = C_\perp \mathcal{V}$$

$\frac{\delta}{\ell} \sim \mathcal{B}$ and $\frac{\lambda}{\ell} \simeq 2$

II

Elastic reconfiguration
$100 < \mathcal{B} < 500$

$$\boxed{\begin{aligned} F_{drag} &\sim \mu U \ell_{app} \\ &\sim \mu U \left[\frac{\mathcal{S}}{\mu U}\right]^{1/2} \\ &\sim (\mu U)^{1/2} \mathcal{S}^{1/2} \end{aligned}}$$

$$\boxed{U \approx \mathcal{V}^{1/2} U_\perp}$$

$$\mathcal{B} \sim \mathcal{V}^{1/2}$$

$\frac{\delta}{\ell} \sim \mathcal{V}^{1/2}$ and $\frac{\lambda}{\ell} \sim \mathcal{V}^{-1/2}$

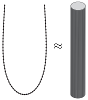

III

Large deformation
$\mathcal{B} > 500$

$$\boxed{F_{drag} \approx 2 C_\parallel \mu U_\parallel \ell}$$

$$\boxed{U \approx U_\parallel}$$

$$\mathcal{B} = C_\parallel \mathcal{V}$$

$\frac{\delta}{\ell} \simeq 1$ and $\frac{\lambda}{\ell} \simeq$ small < 1

Steady shape of the fiber

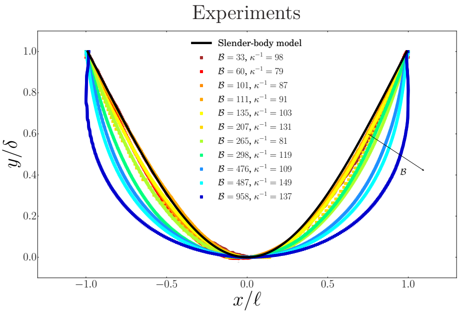

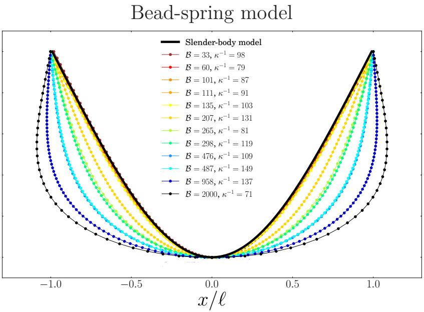

Steady shape scaled by δ

Evolution from a "V" to a "U" shape as $\mathcal{B}$ increased.
$\Rightarrow$ Good agreement between experiments and simulations

Amplitude and end-to-end distance

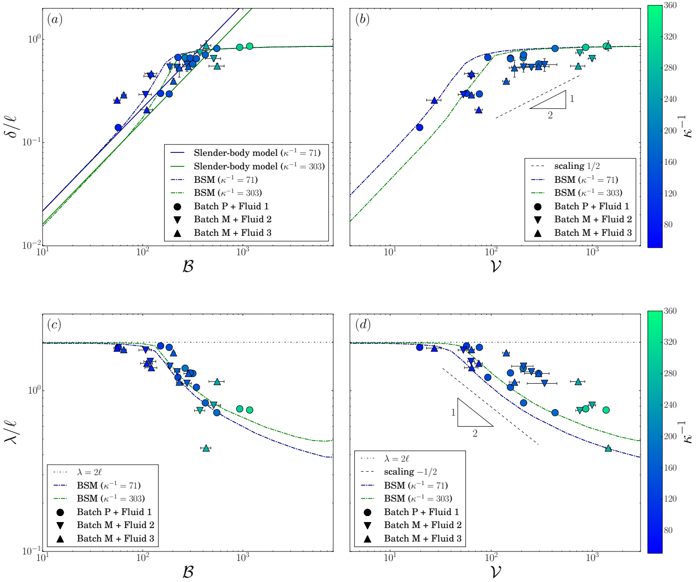

Velocity

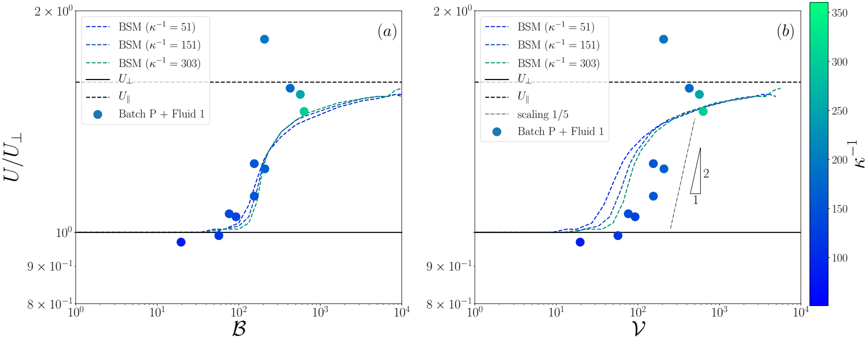

Scaled velocity, $U/U_\perp$, versus $\mathcal{B}$ and $\mathcal{V}$ for different κ^{-1}

- Weak deformation: $U \simeq U_\perp$
- Reconfiguration: $U/U_\perp \sim \mathcal{V}^{1/2}(\kappa^{-1})$
- Saturation: $U = 1.6U_\perp$

Dimensionless drag versus dimensionless velocity

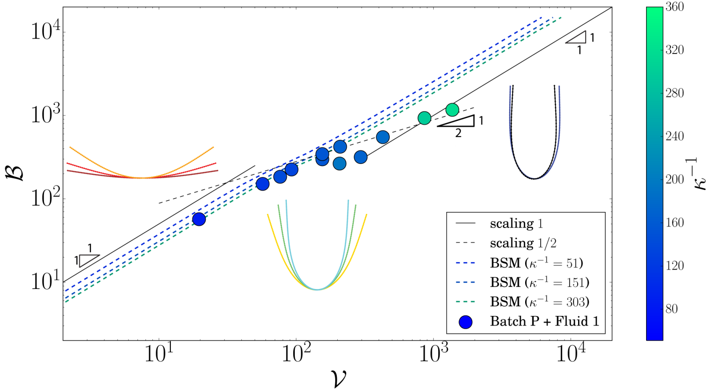

Dimensionless drag, $\mathcal{B}$, versus dimensionless velocity, $\mathcal{V}$, for different κ^{-1}

- Weak deformation: $\mathcal{B} \approx C_{\perp}\mathcal{V}$
- Reconfiguration: $\mathcal{B} \sim \mathcal{V}^{1/2}$
- Saturation: $\mathcal{B} \approx C_{\parallel}\mathcal{V}$

Conclusion

- Joint experimental, analytical, and numerical investigation of the equilibrium deformation of a flexible fiber settling in a quiescent viscous fluid
- Identification of **3 regimes**:
  - I **weak deformation** ($\mathcal{B} < 100$)
  - II **intermediate elastic reconfiguration** ($100 < \mathcal{B} < 500$)
  - III **large deformation**(saturation) ($\mathcal{B} > 500$)

Conclusion & perspectives

Conclusion

Sedimentation of cloud of particles in cellular flows

- Joint experimental and numerical investigation on the cloud dynamic
- Success of Stokeslets in viscous regime and Oseenlets in weak inertia regime
- The cloud zigzags around vortices
- The cloud aspect ratio changes (vertical or horizontal expansion)
- The leakage is amplified by cellular flows
- The life-time is reduced by cellular flows

B. Marchetti *et al.*, JFM (in preparation)

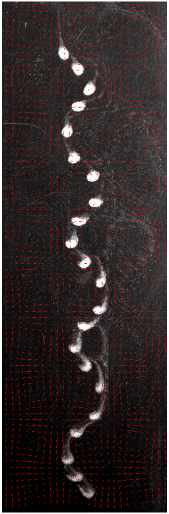

Conclusion

Sedimentation of flexible fibers

- Joint experimental, analytical, and numerical investigation of the equilibrium deformation
- The identification of three regimes (weak deformation I, intermediate elastic reconfiguration II and large deformation III)

B. Marchetti *et al.*, Phys. Rev. Fluids (Accepted)

- Study of the dynamic of deformation of fiber

  $\rightarrow$ time to reach the final steady shape

V. Raspa *et al.* (in preparation)

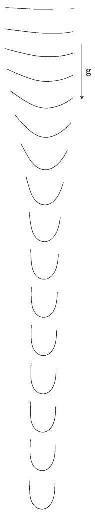

Perspectives

Sedimentation of cloud of particles

- Effect of an increase of the Reynolds number of the flow $(Re_k > 15)$
- Sedimentation of a dilute suspension in cellular flows

Sedimentation of flexible fibers in cellular flows

- Individual fiber or a "cloud" of fibers
- Preliminary study: flexible fiber in a shearing flow
  $\rightarrow$ contribution of the flow in the fiber deformation

Thank you for your attention

This work has been undertaken under the auspices of the ANR project "Collective Dynamics of Settling Particles In Turbulence" (ANR-12-BS09-0017-01), the 'Laboratoire d'Excellence Mécanique et Complexité' (ANR-11-LABX-0092), the Excellence Initiative of Aix-Marseille University - A*MIDEX (ANR-11-IDEX-0001-02) funded by the French Government "Investissements d'Avenir programme"

Influence of collectif effects

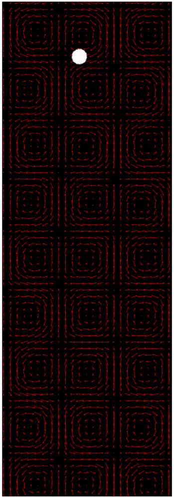

Figure 20: Numerical simulation with interaction between particles (accelerated x8)

$$N_0 \approx 2500$$
$$P \approx 0.02$$
$$W \approx 0.02$$
$$St_p < 3\ 10^{-4}$$
$$Re_k \approx 0.7$$
$$Re_a = 2\ 10^{-4}$$

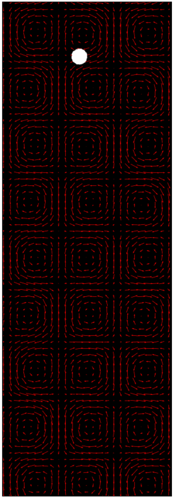

Figure 21: Numerical simulation without interaction between particles (accelerated x8)

Influence of 3D flow field

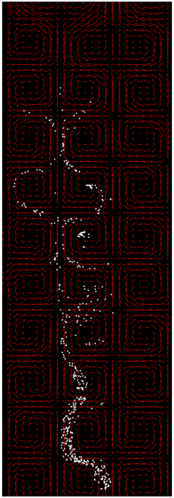

Figure 22: Numerical simulation with 3D flow field

$$N_0 \approx 500$$
$$P \approx 0.03$$
$$W \approx 0.05$$
$$St_p < 4\ 10^{-3}$$
$$Re_k \approx 13.6$$
$$Re_a = 2\ 10^{-2}$$

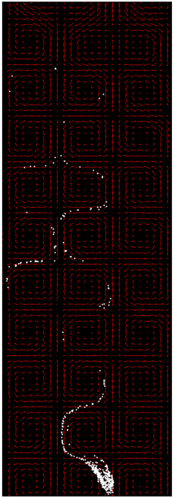

Figure 23: Numerical simulation with 2D flow field

3D trajectory of the cloud

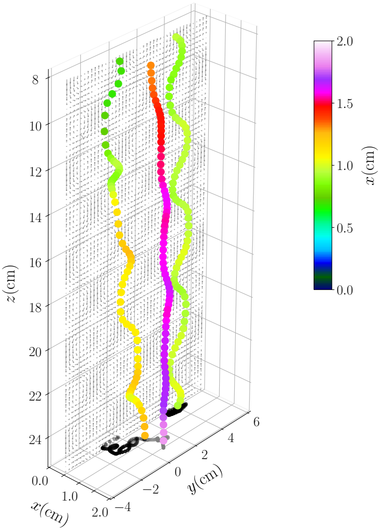

Oseen interactions

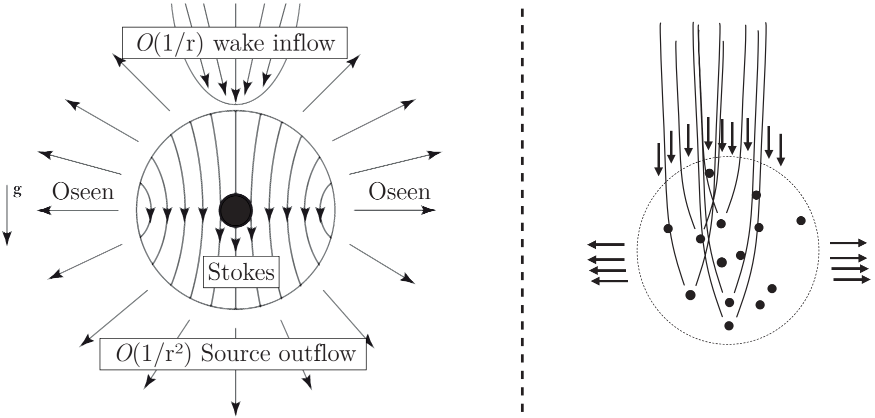

Figure 24: Oseen interactions for an isolated sphere and for suspension(**source**: Subramanian and Koch, JFM (2008))

Interaction with vortices

Perturbed streamlines together with the original PIV flow fields

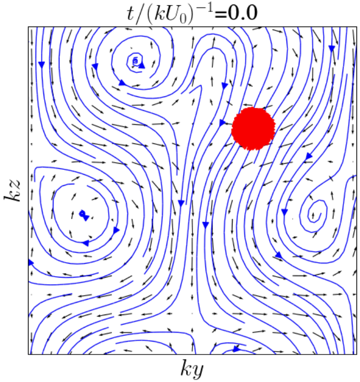

Figure 25: Stokeslet $N_0 = 2500$ (accelerated x3)

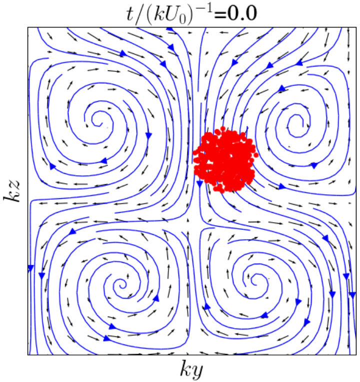

Figure 26: Oseenlet $N_0 = 500$

Leakage of particles

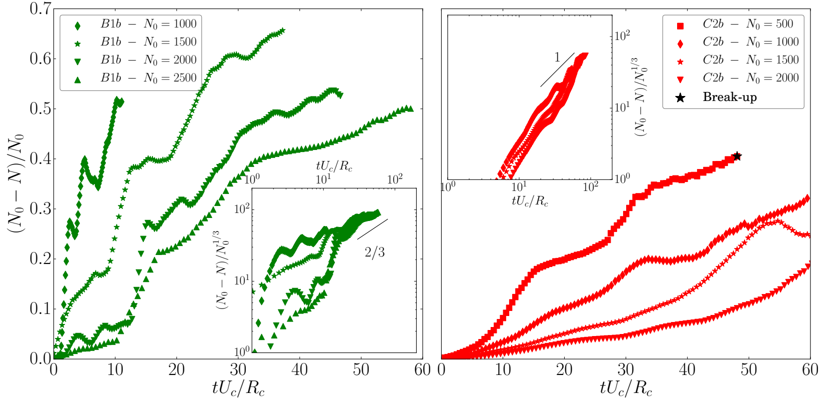

Particle leakage from the cloud

- The rate of leakage decreases as N_0 increases
- Normalizing the leakage $N_0 - N$ by $N_0^{1/3}$ produces a collapse of the data

Newell algorithm

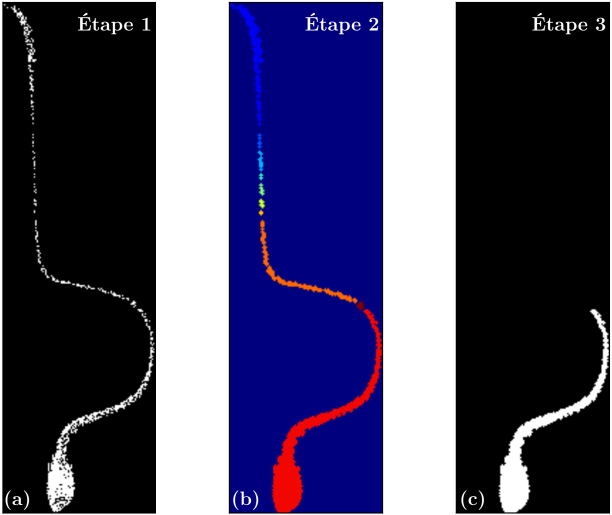

Typical deformation of a rectangular plate

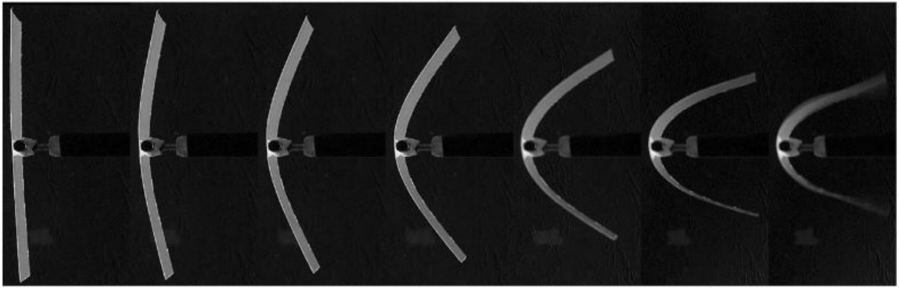

Figure 27: Top view photographs of the deforming plate subjected to flow velocities of $0,\ 2.4,\ 3.6,\ 5,\ 8.6,\ 14.2$ and $16.6\ m.s^{-1}$ (**source**: Gosselin et *al*, JFM (2010))

Typical deformation of a rectangular plate

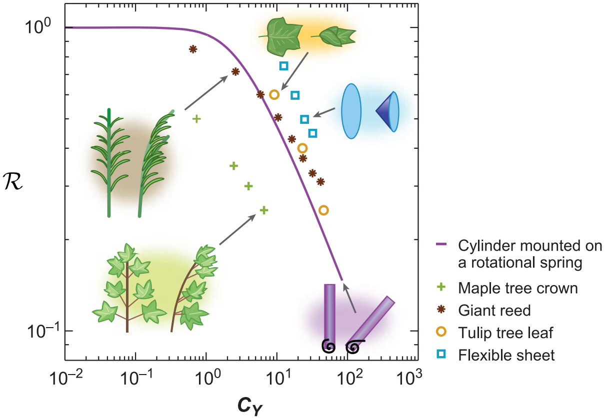

Figure 28: Reconfiguration, with a variation of the drag factor with the Cauchy number (**source**: de Langre et *al*, Ann. Rev. Fluid Mech (2008)

$$F^{drag} \propto U^{2+E_V} \quad C_Y = \frac{\rho_f L^3 U^2}{16 B_f} \quad \mathcal{R} = \frac{F^{drag}}{\frac{1}{2}\rho_f LWCU^2}$$

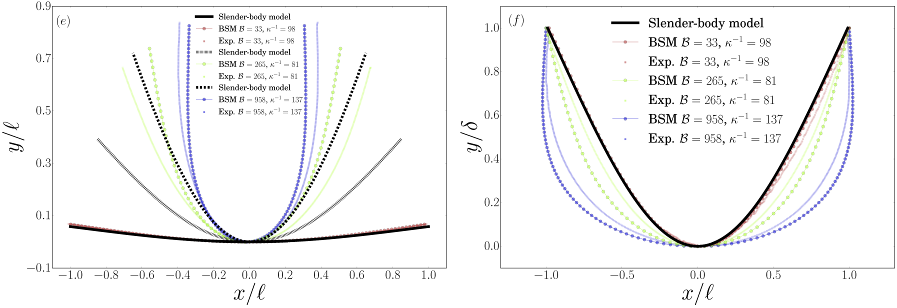

Figure 29: Comparison between experimental and numerical shapes for different $\mathcal{B}$ and κ^{-1}

Shape along the time

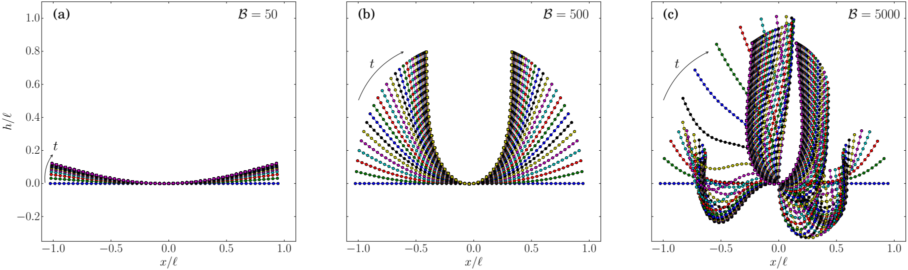

Figure 30: Shape along the time for different $\mathcal{B}$

Velocity and deformation along the time

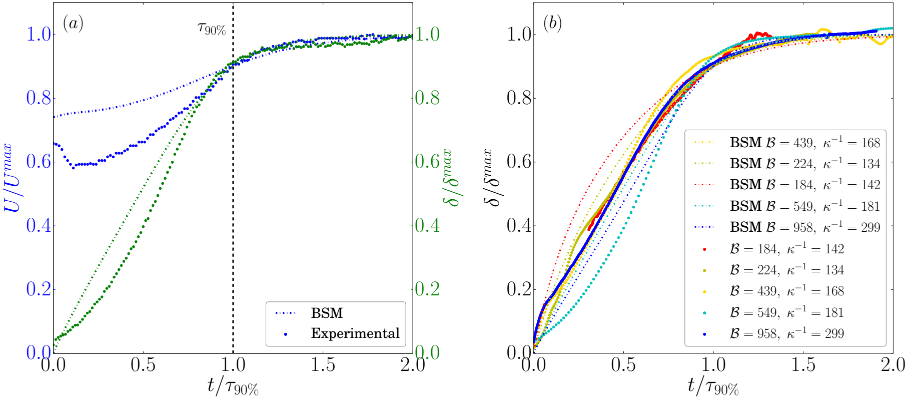

Figure 31: U/U^{max} and δ/δ^{max} along the time

Time, $\tau_{90\%}$ to reach the steady shape

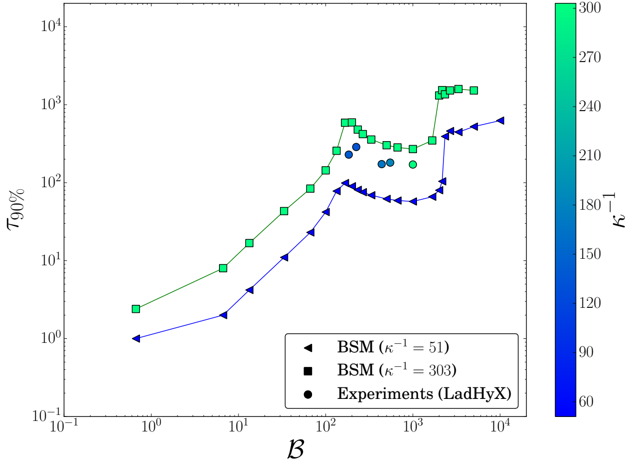

Figure 32: $\tau_{90\%}$ for different value of $\mathcal{B}$ and κ^{-1}

Fibers settling with different initial angle

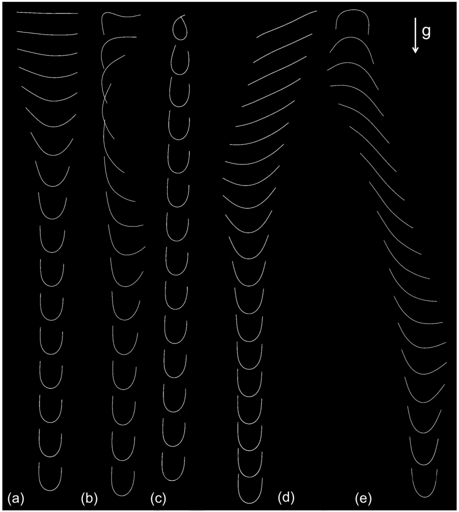

Figure 33: Experimental results from V. Raspa and C. Duprat (LadHyX)

Slender body analytical deflection for small deformation of a long filament perpendicular to gravity

Net external force density along a slender body in a viscous fluid

$$f^{ext} = \frac{2\pi\mu U_{\perp}}{ln(\kappa)^2}\left(2ln(2) - 2 - ln\left[1 - (\frac{x}{\ell})^2\right]\right)$$

Final and stationary deformation by solving Euler-Bernoulli equation

$$EI\frac{d^4y}{dx^4} = f^{ext} \text{ (with } y(0) = 0,\ y'(0) = 0,\ y''(\ell) = 0,\ y'''(\ell) = 0)$$

$$\therefore$$

$$y(x) = -\frac{1}{24}[(1+x)^4 ln(1+x) + (1-x)^4 ln(1-x) - (\frac{3}{16} + 2ln(2))x^4 - (1+12ln(2))x^2]$$

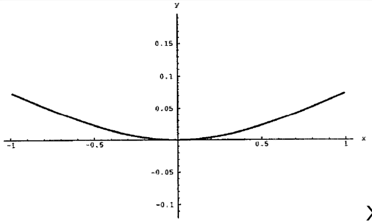

Xu and Nadim, PoF (1994)